

## Supplementary Information

# Ultra-high-aspect-ratio structures through silicon using infrared laser pulses focused with axicon-lens doublets

Niladri Ganguly<sup>1</sup>, Pol Sopena<sup>1</sup>, and David Grojo<sup>1\*</sup>

<sup>1</sup>Aix-Marseille University, CNRS, LP3 UMR 7341, F-13288 Marseille, France

\* Correspondence to: David Grojo: [david.grojo@univ-amu.fr](mailto:david.grojo@univ-amu.fr)

### Authors contact details:

1<sup>st</sup> Author: [niladri.GANGULY@univ-amu.fr](mailto:niladri.GANGULY@univ-amu.fr)

2<sup>nd</sup> Author: [pol.SOPENA-MARTINEZ@univ-amu.fr](mailto:pol.SOPENA-MARTINEZ@univ-amu.fr)

Figures: S1 – S8

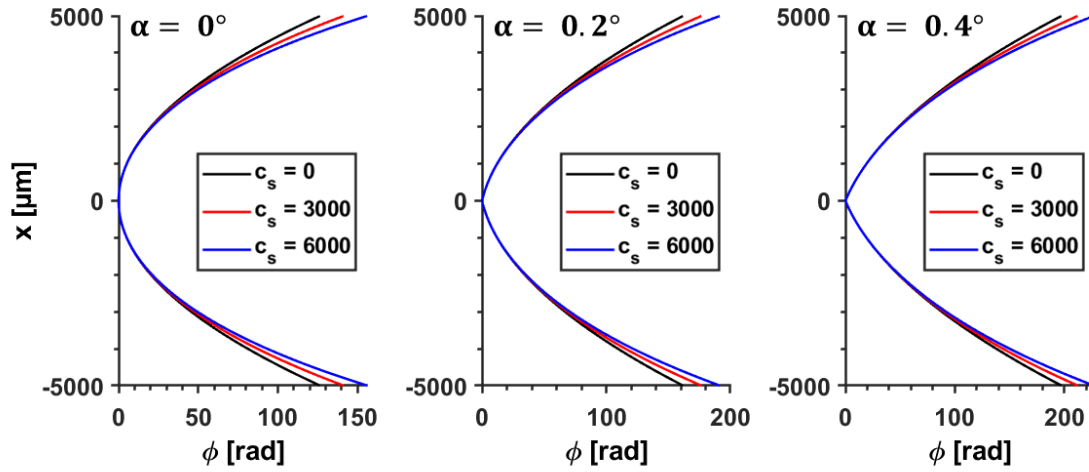


**Fig.S1:** Accounted phase-profiles in the simulations for different combinations of axicon-lens doublets. Each phase-profile adds three contributions: a spherical-phase describing focusing with lens of focal length  $f = 400$  mm, a non-spherical curvature to describe the effect of spherical aberration with strength  $c_s$ , and a conical phase to describe the effect of an axicon of base-angle  $\alpha = 2^\circ$ .

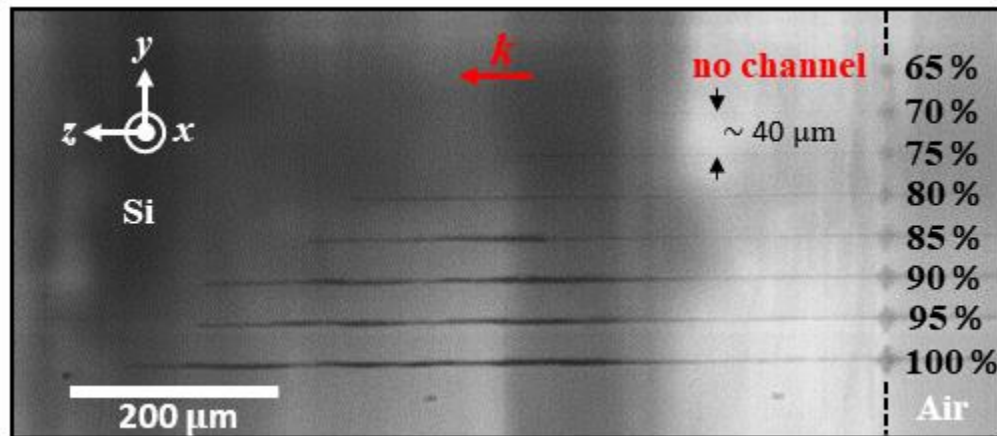


**Fig.S2:** Induced microchannel modifications with pseudo-Bessel micro-beams inside c-Si at varying pulse energy ( $E$ ). The modifications are written with repeated irradiations ( $N = 20,000$ ) of picosecond pulses. Focusing depth is fixed at  $600 \mu\text{m}$  under the wafer surface (indicated by black dashed line). The apparent modification threshold is estimated to be  $12.9 \mu\text{J}$  (at 70%). ‘ $k$ ’ indicates the writing laser propagation direction. Separation between the adjacent microchannels is  $40 \mu\text{m}$ .

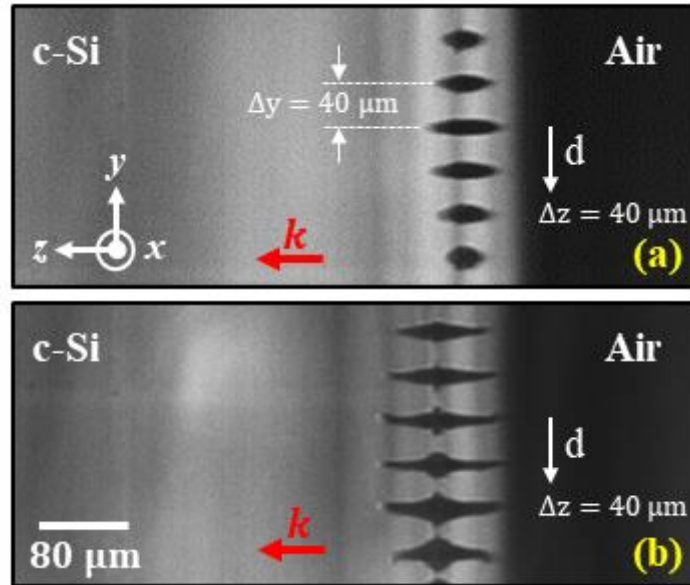


**Fig.S3:** Modification responses at varying depth ( $d$ ) inside c-Si when focusing – (a) picosecond laser pulses with an objective lens of NA 0.45, and (b) femtosecond pseudo-Bessel beam with an axicon-lens doublet (objective: NA 0.45, axicon:  $\alpha = 2^\circ$ ). Laser conditions:  $E = 18.5 \mu\text{J}$ , and  $N = 20,000$  pulses. Both cases show no deep-bulk-modifications except damages in the vicinity of the surface entrance.  $\Delta y$  and  $\Delta z$  are the laser-writing intervals along  $y$  and  $z$  directions, respectively.

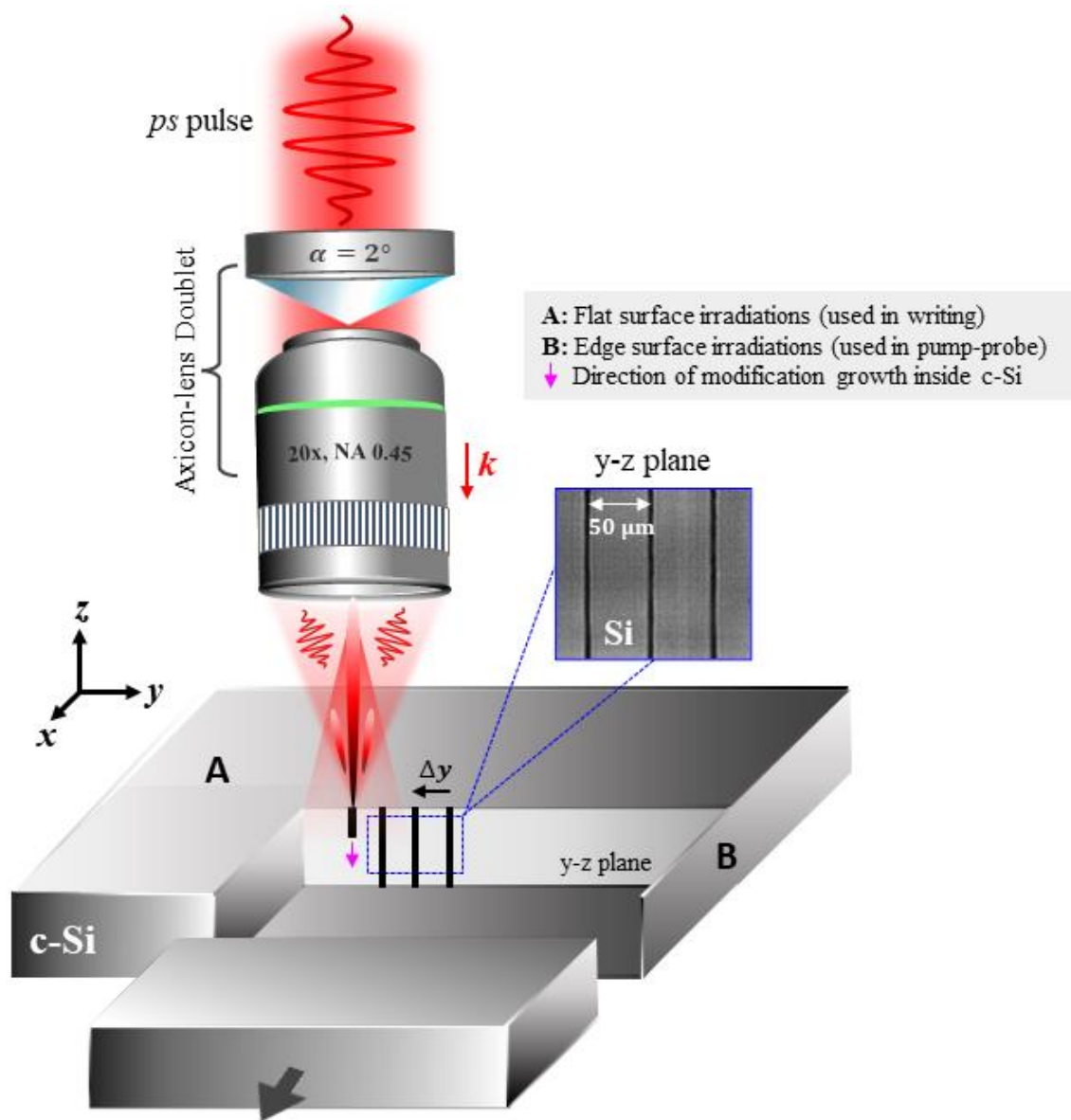


**Fig.S4:** Schematic of the writing arrangement to fabricate high-aspect-ratio microchannels through c-Si with percussion writing modality. The top flat surface (A) of the sample is considered for laser-irradiations. Inset: Cross-sectional view (y-z plane) of the produced structures inside c-Si as observed by infrared transmission microscopy system.  $\Delta y$  indicates the separation between adjacent microchannels set at 50  $\mu\text{m}$  in this specific case. More configuration details are given in the main text (see section ‘*Experimental setup*’).

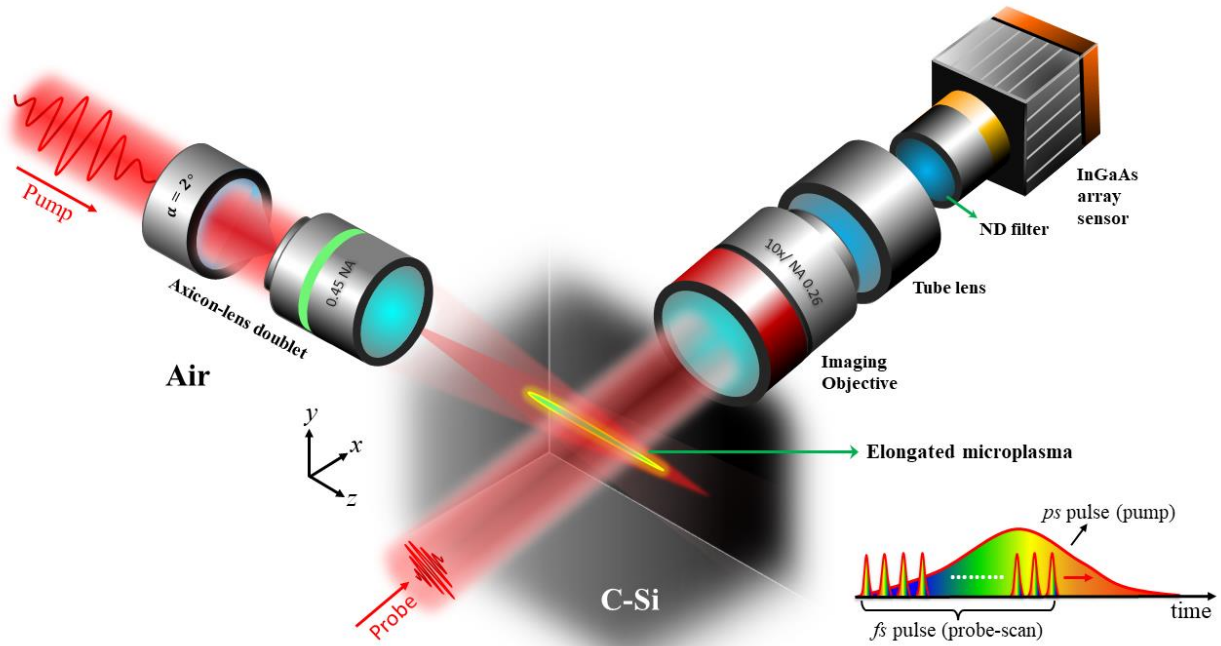
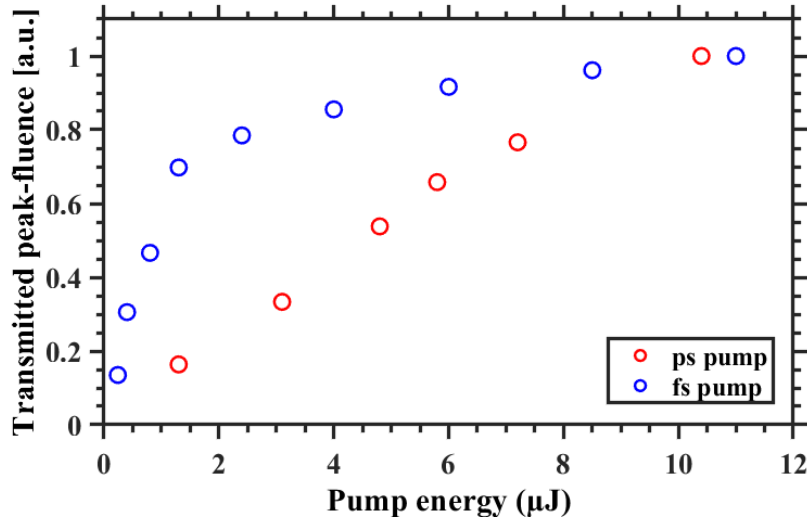
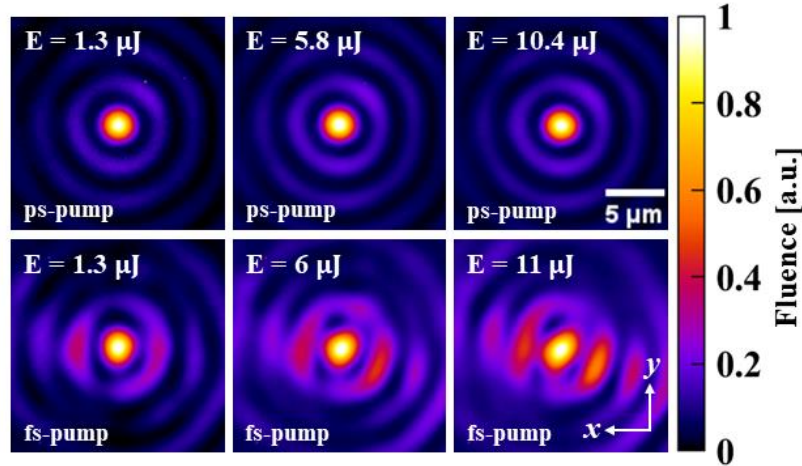


**Fig.S5:** Schematic of the experimental geometry used for pump-probe measurement to study the ionized-microplasma associated energy coupling of the pseudo-Bessel micro-beams within the bulk of c-Si. The delayed fs-probe pulse is used for the *in-situ* observations of the spatio-temporal dynamics of the elongated microplasma channels induced by the picosecond and femtosecond pumps, respectively. The narrow 1-mm thick edge surface (B) of the sample is considered for laser-irradiations. More configuration details are given in the main text (see section ‘*Experimental setup*’).



(a)



(b)

**Fig.S6:** (a) Transmitted peak-fluence (normalized to maximum) as a function of the pump energy ( $E$ ), for different pump-irradiation conditions. Measured values correspond to the peak-signal levels of the pseudo-Bessel beam-focus as imaged with a microscope at the flat back surface of the 1-mm thick c-Si sample. While the picosecond pump exhibits an almost linear increase of the peak-fluence, the femtosecond pump experiences an important clamping due to strong nonlinear pulse-distortion and plasma effects inside c-Si. (b) Corresponding profile images of the pseudo-Bessel beam-focus measured at the flat back surface of the c-Si wafer, showcasing the beam-distortions in the case of the femtosecond pump at high  $E$  values ( $\sim 11 \mu\text{J}$ ), whereas the beam profiles associated to the picosecond pump is almost unaffected with the equivalently increasing value of  $E$ . These results confirm that the picosecond pump is less prone to nonlinear interaction effects inside c-Si. Each image is normalized with respect to its peak-fluence level.

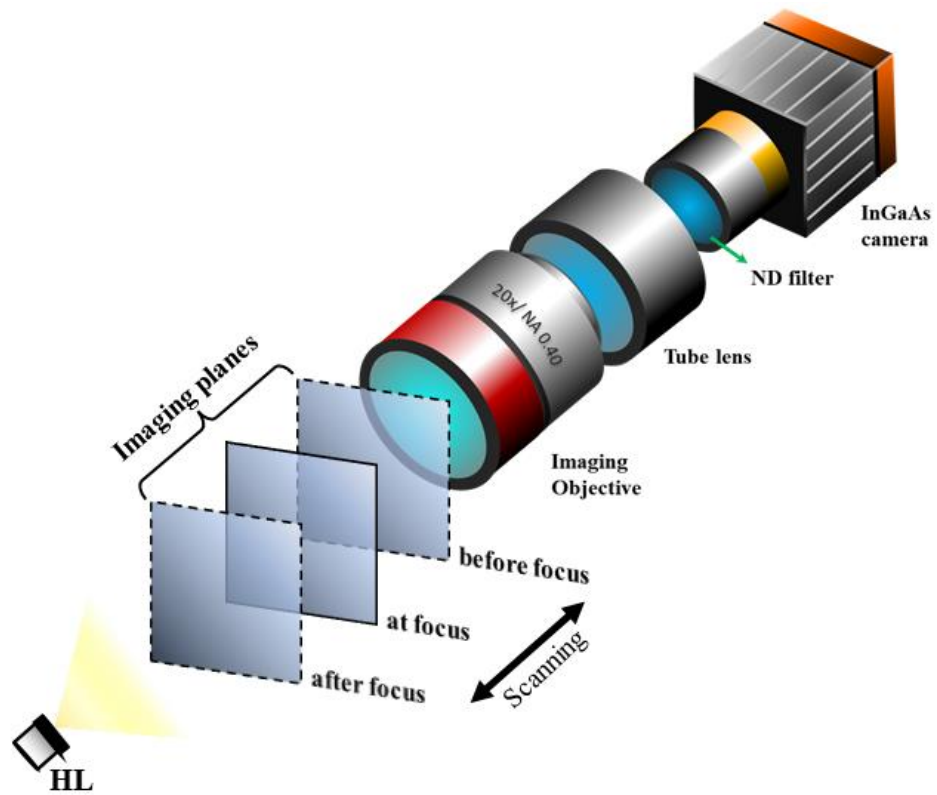


**Fig.S7:** Schematic of the high-resolution infrared transmission microscopy system to record shadow-images of the microchannels formed in the bulk of c-Si. Shadow-images are taken with 20x magnification, at different imaging-focusing-depths to retrieve useful optical information linked with the written structures. Illumination source is a halogen lamp (HL).

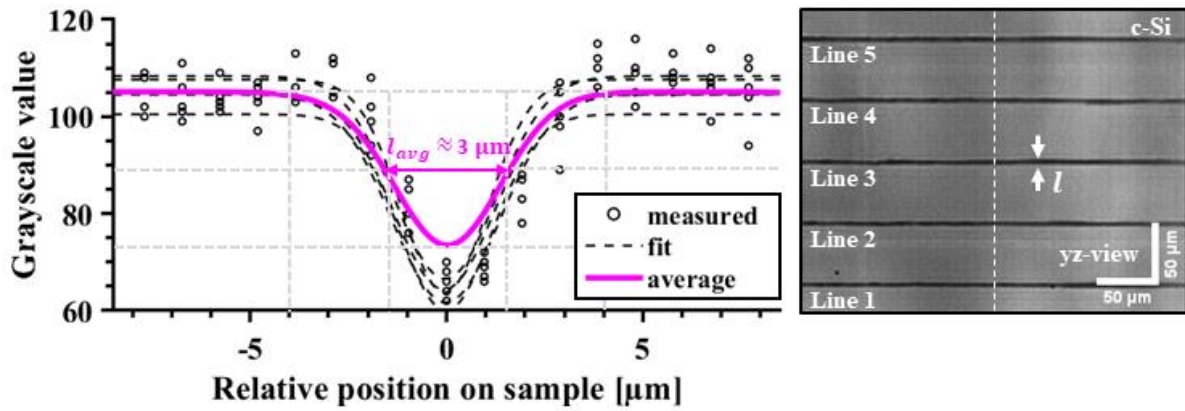


**Fig.S8:** Lateral profiles of the written microchannels inside c-Si obtained by focusing 50-ps infrared laser pulses using axicon-lens doublet under identical condition at  $d = 600 \mu\text{m}$ ,  $E = 18.5 \mu\text{J}$  and  $N = 20,000$  pulses. Inset represents the measured IR transmission microscopy image of those reproducible microchannels. Only the central part of the fabricated channels is shown here.